First publ. in: European Journal of Cell Biology 79 (200), pp. 642-652

Sub-second quenched-flow/X-ray microanalysis shows rapid Ca^{2+} mobilization from cortical stores paralleled by Ca^{2+} influx during synchronous exocytosis in *Paramecium* cells

Martin Hardt, Helmut Plattner[1)]

Department of Biology, University of Konstanz, 78457 Konstanz/Germany

Received March 17, 2000
Received in revised version May 12, 2000
Accepted May 24, 2000

Calcium – exocytosis – microanalysis – Paramecium – secretion

Though only actual local free Ca^{2+} concentrations, $[Ca^{2+}]$, rather than total Ca concentrations, [Ca], govern cellular responses, analysis of total calcium fluxes would be important to fully understand the very complex Ca^{2+} dynamics during cell stimulation. Using *Paramecium* cells we analyzed Ca^{2+} mobilization from cortical stores during synchronous ($\leq$80 ms) exocytosis stimulation, by quenched-flow/cryofixation, freeze-substitution (modified for Ca retention) and X-ray microanalysis which registers total calcium concentrations, [Ca]. When the extracellular free calcium concentration, $[Ca^{2+}]_e$, is adjusted to $\sim$30 nM, i.e. slightly below the normal free intracellular calcium concentration, $[Ca^{2+}]_i = 65$ nM, exocytosis stimulation causes release of 52% of calcium from stores within 80 ms. At higher extracellular calcium concentration, $[Ca^{2+}]_e = 500$ µM, Ca^{2+} release is counterbalanced by influx into stores within the first 80 ms, followed by decline of total calcium, [Ca], in stores to 21% of basal values within 1 s. This includes the time required for endocytosis coupling (350 ms), another Ca^{2+}-dependent process. To confirm that Ca^{2+} mobilization from stores is superimposed by rapid Ca^{2+} influx and/or uptake into stores, we substituted Sr^{2+} for Ca^{2+} in the medium for 500 ms, followed by 80 ms stimulation. This reveals reduced Ca signals, but strong Sr signals in stores. During stimulation, Ca^{2+} is spilled over preformed exocytosis sites, particularly with increasing extracellular free calcium, $[Ca^{2+}]_e$. Cortically enriched mitochondria rapidly gain Ca signals during stimulation. Balance calculations indicate that total Ca^{2+} flux largely exceeds values of intracellular free calcium concentrations locally required for exocytosis (as determined previously). Our approach and some of our findings appear relevant also for some other secretory systems.

Abbreviations. ASs Alveolar sacs. – [Ca] Total calcium concentration. – $[Ca^{2+}]$ Free calcium concentration. – EDX Energy-dispersive X-ray microanalysis.

Introduction

Ca^{2+} acts as a key regulator for a variety of cell functions. During stimulation of exocytosis, cortical Ca^{2+} may increase by release from cortical stores and/or influx from the outside medium into the cytosol (Berridge, 1998; Rutter et al., 1998; Barritt, 1999; Mackrill, 1999). However, in many systems there are still some enigmatic aspects, especially with regard to cortical Ca stores. Unclear are, e.g., the mode of their physical and/or functional coupling to the plasma membrane, and how their mobilization may be rapidly counteracted by a superimposed Ca^{2+} influx. Ca^{2+} influx coupled to store depletion has been designated "capacitative", or "store-operated Ca^{2+} influx" (SOC), respectively, depending on the activation mechanism (Berridge, 1998; Barritt, 1999; Mackrill, 1999). The resulting currents, like I_{SOC}, serve to enhance cortical cytosolic $[Ca^{2+}]_i$, while stores may be refilled only on a larger time scale by a SERCA-type Ca^{2+} pump (Clapham, 1995; Berridge, 1998). Concomitantly, cortical Ca stores are also endowed with a SERCA pump (Meldolesi and Villa, 1993; Inesi and Sagara, 1994).

In the ciliated protozoan, *Paramecium*, flat "alveolar sacs" (ASs) are intimately associated with the plasma membrane. ASs line almost the entire cell surface, with structural links to the cell membrane, thus forming a subplasmalemmal space of

[1)] Prof. Dr. Helmut Plattner, Department of Biology, University of Konstanz, D-78457 Konstanz/Germany, e-mail: helmut.plattner@uni-konstanz.de, Fax: +49 7531 88 2245.

only ~15 nm in width (Plattner et al., 1991). ASs are dynamic cortical Ca stores (Stelly et al., 1991, 1995; Knoll et al., 1993). In their appearance they are similar to subsurface cisternae in some neuronal systems (Metuzals et al., 1997; Berridge, 1998) and in pituitary gonadotrophs (Tse et al., 1997). So far ASs have been characterized in part by widely different methods. These include *(i)* ATP-dependent $^{45}Ca^{2+}$ uptake after isolation (Stelly, 1991; Länge et al., 1995), *(ii)* in situ Ca localization by electron spectroscopic imaging, ESI (Knoll et al., 1993), and secondary ion mass spectroscopy, SIMS (Stelly et al., 1995), *(iii)* localization of a calsequestrin-like protein (Plattner et al., 1997b), *(iv)* cloning and localization of a SERCA-type pump (Hauser et al., 1998), *(v)* biochemical and pharmacological characterization of phospho-intermediate formation (Kissmehl et al., 1998), and, finally, *(vi)* activation of Ca^{2+} release by caffeine (Klauke and Plattner, 1998). No second messengers or Ca^{2+}-induced Ca^{2+} release (CICR) could be found (Länge et al., 1995; Zhou et al., 1995).

During stimulation of trichocyst exocytosis by the polyamine secretagogue aminoethyldextran, AED (Plattner et al., 1985), cortical Ca^{2+} signals occur also in absence of Ca_e^{2+} (Erxleben et al., 1997; Klauke and Plattner, 1997) and total Ca in ASs has been shown by the SIMS method to decrease (Stelly et al., 1995), though with rather limited temporal and spatial resolution due to inherent limitations of this method. Stimulation at $[Ca^{2+}]_e \leq [Ca^{2+}]_i^{rest}$ (~50 nM (Klauke and Plattner, 1997)) still activates ~40% of all exocytosis sites (Erxleben et al., 1997; Plattner et al., 1997a), while full activation requires additional Ca^{2+} influx (Kerboeuf and Cohen, 1990; Plattner et al., 1997a) which results in stronger cortical $[Ca^{2+}]_i^{act}$ signals (Klauke and Plattner, 1997). At $[Ca^{2+}]_e \geq 50$ μM, AED activates all of the $\sim 10^3$ preformed exocytosis sites synchronously within only 80 ms, followed by membrane resealing during 350 ms (Knoll et al., 1991). Ca^{2+} release from ASs, superimposed by Ca^{2+} influx, is also induced by caffeine (Klauke and Plattner, 1998). Therefore, we now looked for a SOC mechanism in our system.

The precise time course of exo-endocytosis coupling in our system was previously established by quenched-flow/cryofixation and electron microscopy (EM) analysis (Knoll et al., 1991). This methodology, combined with freeze-substitution adapted for Ca retention, now allowed us quantitative energy dispersive X-ray microanalysis (EDX) on the EM level. With this method one can determine total Ca concentrations, [Ca], in stores and changes in [Ca] occurring during stimulation. We stress that this method measures total [Ca]. By manipulating $[Ca^{2+}]_e$ or by substituting Sr^{2+} for Ca_e^{2+} during AED stimulation, we can now establish some new aspects: *(i)* Ca^{2+} mobilization from ASs is a primary step which *(ii)* is superimposed by a Ca^{2+} (Sr^{2+}) influx into stores. *(iii)* There seems to be a site-directed Ca^{2+} flux over preformed exocytosis sites, *(iv)* accompanied by swift attenuation towards the cell interior and rapid transient uptake into cortical mitochondria.

Considering profound uncertainties in the regulation of crosstalk between cortical stores and the cell surface (Putney, 1999), our analyses may be an important methodical approach. Our findings may serve as a paradigm for detailed analyses of Ca^{2+} signals in some other "lower" eukaryotes, like parasitic members of the group of Apicomplexans which rely on similar Ca^{2+} signals for exocytosis during host cell penetration (Carruthers and Sibley, 1999; Ngo et al., 2000).

Materials and methods

Cells and exocytosis stimulation

Paramecium tetraurelia (wild-type strain 7S) cultures were grown axenically at 25 °C until early stationary phase. Prior to experiments cells were washed and kept starving overnight in Pipes buffer (5 mM, pH 7) containing $CaCl_2$ and KCl, 1 mM and 0.1 mM each, respectively, as indicated. Paramecia were concentrated by low speed centrifugation to 3.5 to 8×10^4 cells/ml and tested for exocytosis competence. Exocytosis was triggered by the polyamine secretagogue, AED (0.01%) under light microscope control and scaled from "−" to "+++" (0 to 100% exocytosis) as indicated elsewhere (Plattner et al., 1985; Knoll et al., 1991; Plattner et al., 1997a).

Concentrations of free divalent cations (Ca^{2+}, Sr^{2+}) were calculated and adjusted, usually by EGTA or in some cases by BAPTA, according to Bers et al. (1994) including binding constants from Schwarzenbach et al. (1957) and Anderegg (1964).

Quenched-flow and freeze-substitution procedure

Cells were spray-frozen into liquid propane (≤ -180 °C) without stimulation or at different times during stimulation of exocytosis, using a quenched-flow apparatus developed in our laboratory (Knoll et al., 1991). This set-up also allows to adjust $[Ca^{2+}]_e$ to different values during 500 ms EGTA application, and to substitute Sr^{2+} for Ca^{2+}, before cells are mixed with AED for different times.

Frozen cells were processed as previously described (Knoll et al., 1991). Briefly, propane was evaporated under vacuum at −100 °C, before cells were subjected to freeze-substitution, 48 h at −80 °C, in dry methanol containing 3% glutaraldehyde, 1% OsO_4, and 250 mM KF to retain Ca (or Sr) in cells, based on previous work (Poenie and Epel, 1987; Knoll et al., 1993). The temperature was raised by 5 °C × h^{-1} and finally cells were embedded in Spurr's resin.

X-ray microanalysis

Sections (500 nm thick) were mounted on Pioloform-coated nickel grids (300 mesh) and analyzed in a EM912 Omega electron microscope (EM) from Zeiss/Leo (Oberkochen, Germany). The characteristics of EM operation were as follows: 80 kV acceleration voltage, tungsten filament, scanning transmission (STEM) imaging mode, spot size = 63 nm for spot measurements, probe diameter = 40 nm for line scans or elemental imaging, emission current ~10 μA, resulting in a calibrated constant dose rate of $\sim 1.2 \times 10^9$ $e^- \times \mu m^{-2} \times s^{-1}$. X-ray signals were collected by a Li-drifted Si-detector (front area 30 mm^2) equipped with an ATW2 atmospheric window, minimal detector-sample distance of ~12.5 mm, 20° to 30° take-off angle. For X-ray signal analysis we used a Link multichannel energy analyzer and Link ISIS 3.00 software (Oxford Instruments, Wiesbaden, Germany). Energy resolution of the detector was 133 eV at 5.9 keV ($Mn_{K\alpha}$).

Ca and Sr signals were analyzed with reference to the element-specific Kα lines (3.691 or 14.143 keV, respectively). $Ca_{K\alpha}$ (3.57 to 3.83 keV) and $Sr_{K\alpha}$ (13.95 to 14.39 keV) count integrals were separated from the continuum, using a digital top-hat filter, and quantified using ISIS software TEMquant (Oxford Instruments). This software allowed digital top-hat filtering and multiple least square fit using default element profiles as references. Systematic errors of the fit due to errors in the default profiles or spectrometer drift were low as compared to random statistical errors. Line scans and $Ca_{K\alpha}$ or $Sr_{K\alpha}$ images were processed with reference to the respective energy windows (3.57 to 3.83 keV for $Ca_{K\alpha}$ and 13.95 to 14.39 keV for $Sr_{K\alpha}$) and non-element-specific X-ray background was subtracted, based on values between 5.11 and 5.38 keV for Ca, or 15.01 to 15.45 keV for Sr, using the Speedmap software from ISIS. The time of irradiation for each measuring point along a scan (collected in 384 s) is very short (equivalent to 128 spots in linear arrangement, allowing for 3 s measuring time per spot), as compared to recordings by spot measurements (100 s), and therefore the resulting signal is relatively weak. Line scans (not to be confused with spectra) reflect the spatial distribution of

counts, contained in the respective energy window, along the scan axis. Considering the short X-ray collection time per unit length, signals considerably fluctuate along a line scan. Density profiles are measured simultaneously along the same axis. This allows to correlate X-ray signals with structural landmarks, even though density signals were considerably stretched to match the X-ray signal distribution.

Element maps were eventually transformed into false-color images to visualize gross Ca or Sr distribution patterns. Line scans and element maps were only used for localization of Ca but not for quantitation.

For resting or AED-stimulated cells, net $Ca_{K\alpha}$ count integrals registered over any subcellular structure were pooled to determine mean values and standard errors (n, N = number of sites or cells analyzed), as established by Chandler (1976) and Dörge et al. (1978). For the different experimental conditions tested at least 5 to 6 measurements were done per analyzed cell compartment, and the resulting data were pooled from at least 5 cells (see Figs. 4 and 5). The collection of these data was usually obtained from 2 to 3 grids. Variation of X-ray counts between preparations may partly arise from varying thickness of sections (determined by interferometrically standardized interference color) and of the Pioloform film, but we have shown that these effects remain low under the experimental conditions used (Hardt and Plattner, 1999).

For in-depth discussion of quantitative EDX methodology, see Warley (1997) and Reimer (1998).

Values indicated for cytosolic [Ca] were always determined at 0.5 μm from a trichocyst docking site. Two widely different types of external standards were used for calibration: *(i)* organic Ca-compounds included in Spurr's resin (Chandler, 1976) purchased from British BioCell (Cardiff, Wales) and distributed by Plano (Wetzlar, Germany), and *(ii)* Ca-exchange beads incubated at different $[Ca^{2+}]$ (DeBruijn, 1981). Method *(i)* was used since it is not liable to Ca loss, while standards from method *(ii)* served to analyze any potential side-effects (like Ca loss or diffusion) since beads can be processed to sections in the same way as paramecia. Both these methods resulted in almost coincident linear calibration curves, with a cut-off at [Ca] = 2 mM (= detection limit). In addition, we controlled [Ca] in the Ca bead standards by atomic absorption or neutron activation (data not shown). As confirmed by these two independent physical methods, the spot mode analysis allowed us the calibration of the $Ca_{K\alpha}$ counts and a direct indication of [Ca] values per unit volume (rather than per kg dry weight) of subcellular structure (Chandler, 1976; Dörge et al., 1978; Hall, 1979). Effects of osmium (mainly fluorescence), though small (<25%), were corrected based on an experimentally determined correction factor (Hardt and Plattner, 1999). Effects of the nickel grid were negligible when spot measurements were executed at distances ≥500 nm from grid bars. Contamination was seen in the images, but it did not impair quantitation since count rates for both, the whole spectrum and the $Ca_{K\alpha}$ or $Sr_{K\alpha}$ energy windows, were constant during our measurements. In previous analyses under identical conditions we have shown that during the entire analysis time (tested up to 125 s) counting rates were constant, even when contamination spots (as in Fig. 2) became visible (see Fig. 7 in the paper by Hardt and Plattner, 1999). Prerequisite was the omission of carbon coating of samples.

In each set of trigger experiments, data were referred to parallel controls (=100%) subjected to the same procedure without stimulation. For statistical analysis we used Sigma-plot 4.0 sofware (Jandel GmbH, Erkrath, Germany). Parametric tests were only used after normality and equal-variance tests were passed.

To summarize, under our conditions we can detect [Ca] ≥ 2 mM, at a spatial resolution which approximately corresponds to the calculated broadening of the primary electron beam in the 500 nm section, i.e. from 63 nm to 72 nm, 90% cut-off, according to Monte Carlo calculations using software by L. Reimer (Münster/W., Germany). Further methodical details are described elsewhere (Hardt and Plattner, 1999).

Concentration units used

We use the terms [Ca] and $[Ca^{2+}]$ to espress concentrations of total (free and structure bound) and of free calcium, respectively. Indices "i" or "e" indicate intracellular and extracellular values, respectively. Designations "rest" and "act" differentiate between values in resting and in activated cells, respectively. Concentrations for $[Ca^{2+}]$ given in "mM" etc. mean millimolar, i.e. mmoles per liter which normally corresponds to mmoles per kg. Since most EDX data were obtained with freeze-dried material, published data are mostly in mmoles per kg dry weight. Since we analyzed embedded cells we prefer to refer our values to volume; considering that density is ~1, we give our data in mmoles per liter (equivalent to millimolar, mM), unless specified otherwise.

Results

STEM analysis of 500 nm thick sections of resting cells shows cilia and trichocysts docked at the cell membrane (Fig. 1A). $Ca_{K\alpha}$ images reveal selective enrichment of Ca in ASs (Fig. 1B). These are flat sacs closely apposed to the plasma membrane (Fig. 1A). While such images serve to visualize gross Ca distribution, their resolution is poor and quantification is difficult.

Therefore, we performed quantitative spot analyses in precisely cross-cut ASs, followed by statistical analysis. Full spectra have been presented in our methodical paper (Hardt and Plattner, 1999; specifically Fig. 2 for ASs and Fig. 9 for a Ca-standard). Only the relevant part of the spectrum is shown in Fig. 2, where spot measurements and line scans show clear $Ca_{K\alpha}$ signals selectively in ASs. The corresponding densitometric profiles roughly define the outlines of ASs, i.e. their inner and outer membrane, the latter being difficult to resolve from the closely attached plasma membrane. While the subplasmalemmal space is difficult to resolve in STEM images, Ca can be clearly localized to ASs, not only by $Ca_{K\alpha}$ energy line scans, but also by spectra from spot measurements. The probe diameter (63 on top and 72 nm at the bottom of a 500 nm section) is sufficiently smaller than the average thickness of cross-cut ASs of 98.5 ± 11.1 nm (Table I). As Fig. 2 shows for a resting cell, ASs are clearly the only source of intense $Ca_{K\alpha}$ signals, in contrast to cilia, trichocysts (with upper slender "tips" and lower thick "body" portions), and mitochondria. Line scans reveal some Ca signals in ASs, but also in the cytosol underneath, and in a ~50 to 100 nm broad region outside the plasma membrane, i.e. the glycocalyx (Fig. 3). These weak signals can be ascertained only by statistical evaluation. In ASs, absolute $[Ca]_{total}$ according to widely different calibration procedures is 43 mmoles per liter (see "Materials and methods"), while detection limit is ~2 mmoles per liter (Table I). Recall that all values obtained by EDX are total calcium concentrations, [Ca].

Next we addressed mobilization of Ca^{2+} from ASs. First we analyzed cells during AED stimulation in the absence of Ca^{2+} influx. For this purpose we reduced $[Ca^{2+}]_e$ to 50 nM, i.e. close to or slightly below $[Ca^{2+}]_i^{rest}$ in cytosol (Klauke and Plattner, 1997, 1998). In the quenched-flow apparatus, we first mixed the cells with EGTA for 500 ms, before stimulation by AED for 30 or 80 ms, respectively (Fig. 4). When compared to unstimulated controls (normalized to 100%), which were always processed in parallel, $Ca_{K\alpha}$ signals in ASs decreased significantly, with an estimated $t_{1/2}$ ~80 ms. Signals obtained from the cytosol (0.5 μm from a trichocyst docking site) increased by 57% within 30 ms and then decreased. While this indicates a rapid Ca^{2+} wave, with a rapid decay as Ca^{2+} sweeps into the interior of the cell, Ca is simultaneously rapidly and efficiently sequestered into mitochondria whose $Ca_{K\alpha}$ signal is

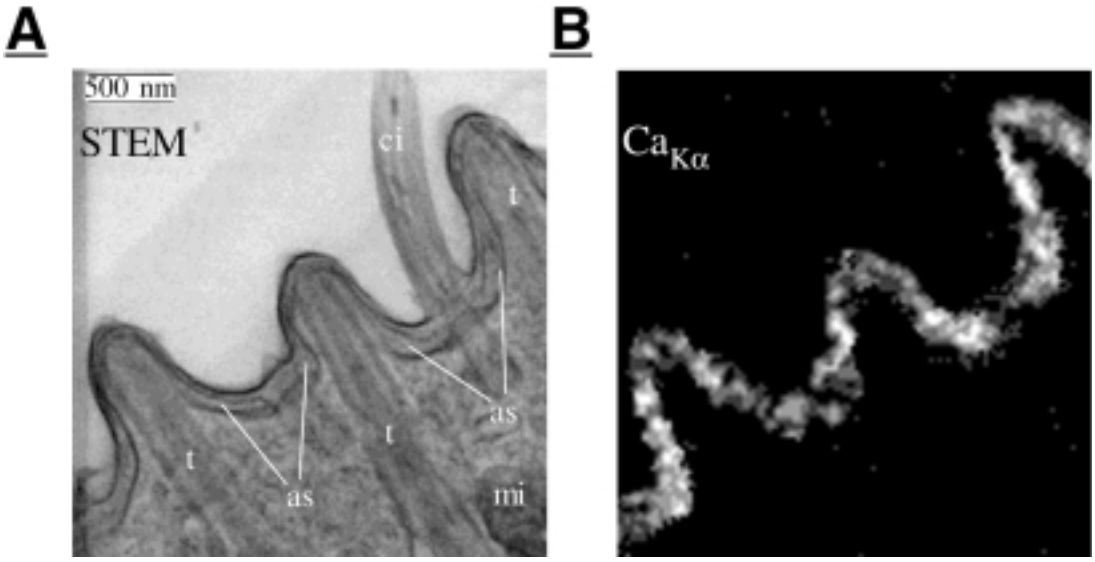

Fig. 1. $Ca_{K\alpha}$ imaging reveals selective Ca enrichment in ASs. STEM (**A**) and corresponding $Ca_{K\alpha}$ image (**B**) of the cortex of an unstimulated cell, processed by quenched-flow/freeze-substitution to retain Ca as described in "Materials and methods". Note selective Ca storage in alveolar sacs (as), while cilia (ci), trichocysts (t), mitochondria (mi), and cytosol yield no signals.

~fivetimes above basal values already 30 ms after AED administration. Most importantly, during AED stimulation, no $Ca_{K\alpha}$ signal increase could be registered in the cytosol directly below alveolar sacs at larger distances from trichocyst docking sites, e.g. when ciliary bases are approached. This implies a site-directed flux of Ca^{2+} during release from ASs.

Next, AED stimulation was repeated at $[Ca^{2+}]_e = 500\ \mu M$ (Fig. 5). Evidently mobilization of Ca^{2+} from ASs was immediately counterbalanced by Ca_e^{2+} influx with immediate uptake into ASs, since their $Ca_{K\alpha}$ signals first slightly increased, though not statistically significantly, within the first 30 ms. The $Ca_{K\alpha}$ signals decrease with an estimated $t_{1/2} \sim 350$ ms. Passage of Ca^{2+} through ASs may facilitate dissipation by a directed flux over trichocyst docking sites, in agreement with Fig. 4. Within 1 s AED stimulation, $Ca_{K\alpha}$ signals in ASs decreased to only 20% of values at t_0. Simultaneously the $Ca_{K\alpha}$ signal rapidly increased in the cytosol (0.5 μm from trichocyst docking sites), to 370% of controls within 30 ms, before values decayed to control levels with $t_{1/2} \sim 100$ ms. Ca^{2+} uptake into mitochondria culminates at 80 ms and still exceeds control values 1 s after AED application. With $[Ca^{2+}]_e = 500\ \mu M$, just as with $[Ca^{2+}]_e = 50$ nM, no cytosolic $Ca_{K\alpha}$ signal can be registered underneath ASs at larger distances from preformed exocytosis sites. This again may indicate a site-directed flux over exocytosis sites and a rapid spread into the remote cytosol, to yield values below detectability.

$Ca_{K\alpha}$ imaging 80 ms after AED stimulation at $[Ca^{2+}]_e = 500\ \mu M$ reveals intense signals not only in ASs (because Ca^{2+} mobilization is immediately superimposed by refilling), but additionally in mitochondria (Fig. 6B) which, in unstimulated controls, display no such signals (Fig. 6A).

Since the immediate transfer of Ca_e^{2+} into cortical stores, which we derive from Figs. 4 and 5, was unexpected, we substituted Sr^{2+} for Ca^{2+} in the medium (Table II). Cells tolerated well low $[Ca^{2+}]_e$ when supplemented with Sr^{2+} (12 h tested) which also supported AED-induced exocytosis (Table II A) and ciliary activity (not shown). Then we briefly exchanged Ca_e^{2+} by Sr_e^{2+}, using appropriate [EGTA], before stimulation by AED which again resulted in massive exocytosis (Table II B). Finally, substitution of Sr^{2+} for Ca^{2+} was done during 80 ms AED stimulation in the quenched-flow apparatus. $Ca_{K\alpha}$ line scans across ASs of controls show weak, but statistically significant Ca signals, in the absence of Sr signals (Fig. 7A, B, without AED), while Fig. 7C, D (with AED) shows $Sr_{K\alpha}$ signals in ASs, this time in absence of Ca signals. Therefore, Sr^{2+} is rapidly (80 ms) transferred into ASs during AED stimulation. This is further supported by $Sr_{K\alpha}$ imaging under similar conditions (Fig. 8). The absence of $Sr_{K\alpha}$ signals from mitochondria after AED stimulation (Fig. 8B), in contrast to the $Ca_{K\alpha}$ signals seen after stimulation in presence of Ca_e^{2+} (Fig. 6), may be explained as follows. Ca^{2+} is mobilized from ASs, paralleled or immediately followed by influx of Sr^{2+} into ASs, before any further dissipation of Sr^{2+} from ASs into the cytosol can occur.

Discussion

Methodical aspects

We knew from high resolution ESI analyses that freeze-substitution in presence of fluoride is appropriate to retain Ca (or Sr) in ASs or, after stimulation, also in the cytosol (Knoll et al., 1993). The same preparation procedure, combined with quenched-flow stimulation, was now combined with EDX.

Our current approach can easily be expanded to Sr substitution experiments, for the following reasons. *(i)* Sr^{2+} has identical physiological effects as Ca^{2+} in our analyses, *(ii)* Sr is well retained by the preparation protocol used, since SrF_2 is only slightly more soluble than CaF_2 (Goodenough and Stenger, 1973), and *(iii)* Sr is well resolvable from Ca in EDX analyses. Previously Ca_e^{2+} has also been successfully replaced by Sr^{2+} for analyzing exo- and endocytosis (Montero et al., 1997).

It is important to note that quantitation of [Ca] in small structures like the ER is a general problem in EDX analysis.

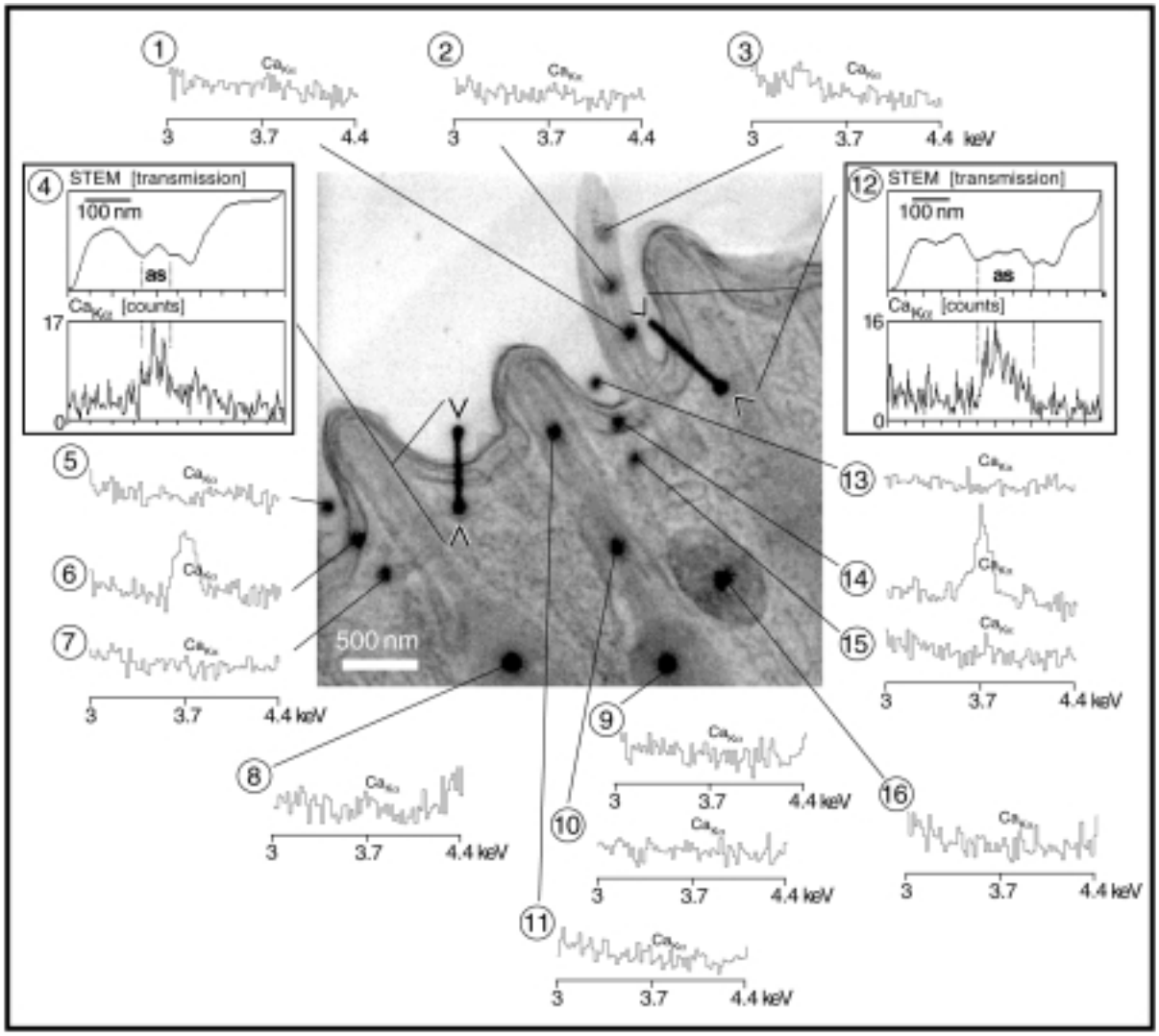

Fig. 2. $Ca_{K\alpha}$ signals are selectively recorded in ASs. STEM image of an unstimulated cell, processed as in Fig. 1, with spot measurements or line scans at sites recognized by black contamination product. Note that $Ca_{K\alpha}$ signals (3.691 keV, within the 3 to 4.4 keV region shown) occur selectively in spectra from alveolar sacs (as, positions 6, 14), while they are absent from any other sites, like cilia (1–3), extracellular medium (5, 13), cytosol (7, 15), trichocysts ("body" portion, 8, 9; "tip" portion, 10, 11) and mitochondria (16). Calibration of counts is the same in all spectra shown here. The peak of the $Ca_{K\alpha}$ signal measured at position 6 is 92 counts above the lowest value in this recording. Line scans through vertically cut alveolar sacs (positions 4, 12) show electron density signals (*upper box*) from alveolar sacs and plasma membrane, and $Ca_{K\alpha}$ signals (*lower box*) in alveolar sacs, with local counts as indicated in the ordinate of positions 4 and 12, respectively.

When the size of the probe exceeds the size of the analyzed structure, the Ca signal appears small and a systematic error of [Ca] would be the consequence (Wendt-Gallitelli and Isenberg, 1991). The fact that the probe size is not only determined by the setting of the EM but also to a large extent by the thickness of the sample therefore imposes a principal limit to EDX studies. However, for our analysis of total [Ca] in ASs this is not relevant since their diameter (98.5 nm) is larger than the probe diameter (63 nm), even when enlargement of the primary electron beam to a calculated 72 nm, at the bottom of a 500 nm section, is taken into account.

In sum, our approach may expand the number of tools available for the analysis of Ca stores and, as recently reviewed (Neher, 1998; Rutter et al., 1998), of Ca^{2+} microdomains. Our method allows to reliably retain calcium and strontium in place, as critically discussed below, even during subsequent plastic embedding, which in turn allows much better structural correlation than freeze-drying.

How reliably is calcium retained by fluoride precipitation during freeze-substitution? Some of the methodical aspects have been experimentally addressed already in detail in a previous methodical paper (Hardt and Plattner, 1999) to which we refer. The following arguments support the feasibility of the method used and the reliability of the novel results achieved.

(i) When we previously had used the same preparation protocol, but in conjunction with high-resolution ESI analysis, we could show selective retention of calcium in ASs in untriggered control cells, as well as occurrence of additional Ca-signals in the cytosolic compartment, 80 ms after AED stimulation (Knoll et al., 1993). Sections (30 to 40 nm thick)

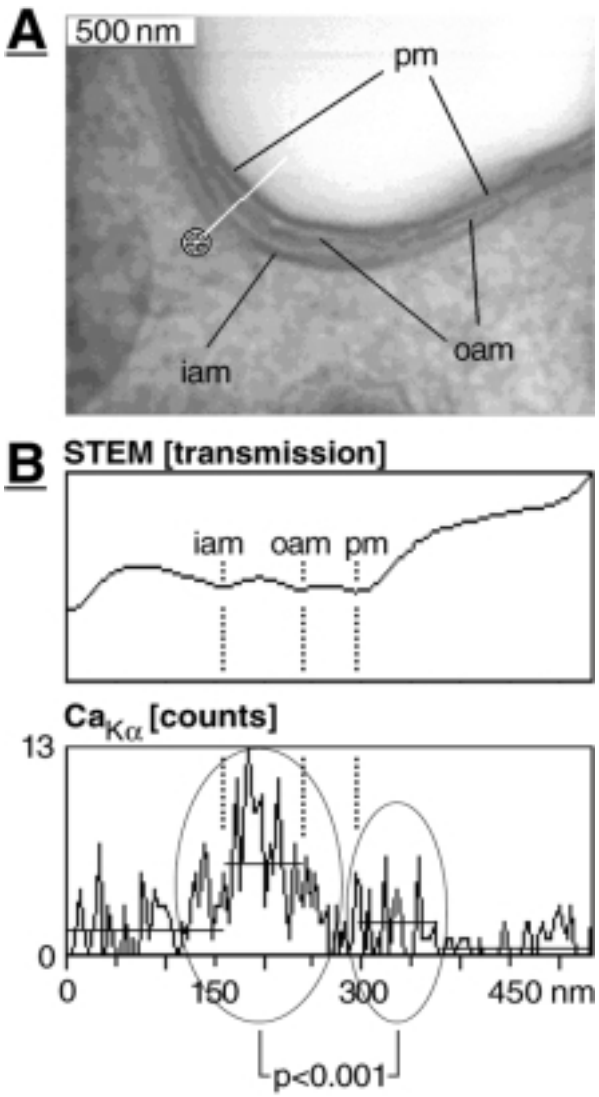

Fig. 3. Detailed STEM and $Ca_{K\alpha}$ line scan analysis of a resting cell prepared as in Fig. 1. The *asterisk* in (**A**) marks start of line scan. Density distribution (*upper box* in (**B**)) indicates positions of inner and outer membrane of alveolar sacs (iam, oam), respectively, and of the plasma membrane (pm). The $Ca_{K\alpha}$ signal distribution (*lower box* in (**B**)) shows significant $Ca_{K\alpha}$ signal in alveolar sacs (between iam and oam), small background in the embedding medium (at >380 nm of the line scan), and slightly higher levels in the cytosol (<150 nm) as well as in the peripheral region adjacent to the plasma membrane (300 to 380 nm) which coincides with the glycocalyx. Horizontal bars = mean values.

Table I. Key-values pertinent to methods.

Width of alveolar sacs, (nm ± s.e.m.)	Mean	98.5 ± 11.1 (N = 10, n = 34)
	Minimum	54.7 ± 4.4 (N = 10, n = 17)
	Maximum	142.3 ± 15.7 (N = 10, n = 17)
Probe diameter, (nm)		63 (spot), 40 nm (line scans)
Resolution of Ca localization, (nm)		72
Minimal [Ca] detected, (mM)		2
$[Ca]_{total}$ in alveolar sacs, (unstimulated), (mM)		43 ± 3.2 (s.e.m.)

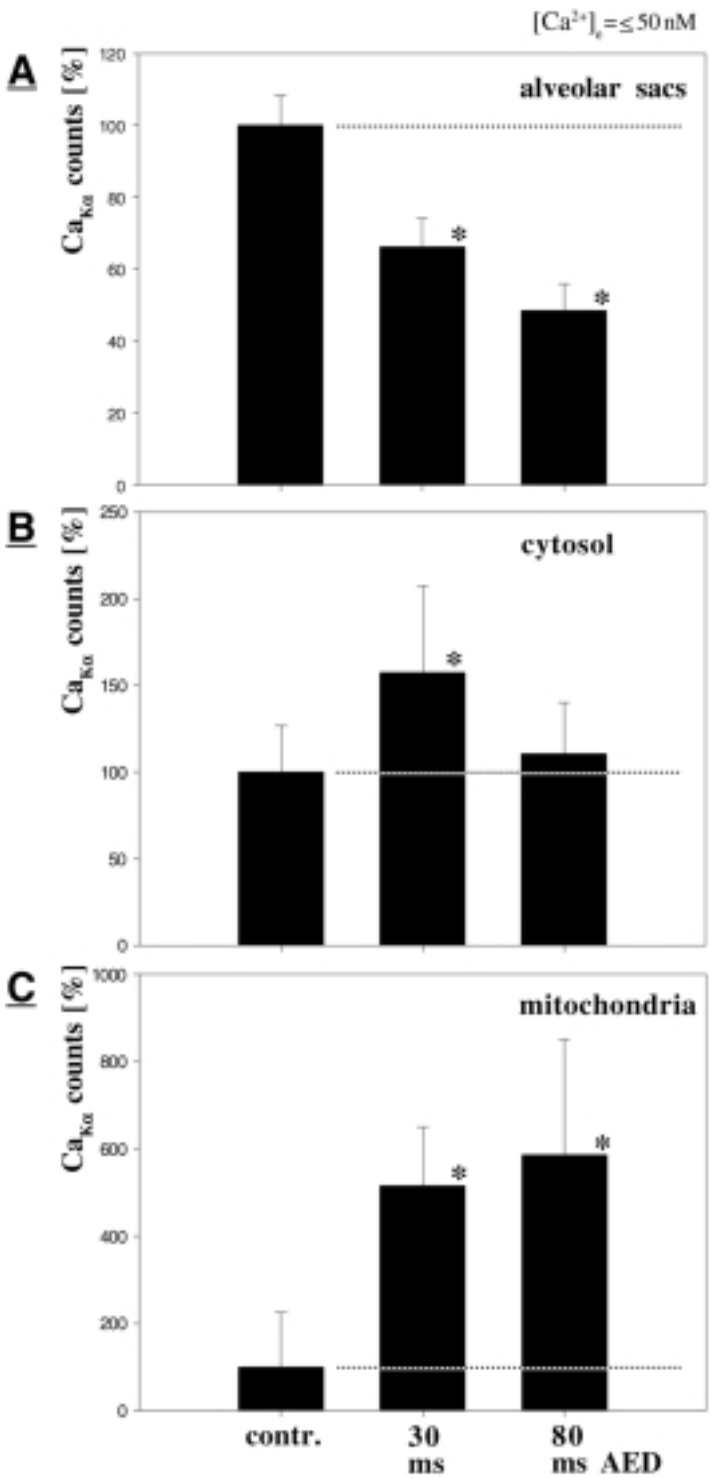

Fig. 4. AED-induced mobilization of Ca^{2+} from alveolar sacs shown at very low $[Ca^{2+}]_e$. Ca^{2+} release from ASs (**A**) is accompanied by spill-over into cytosol (**B**) and rapid upake into mitochondria (**C**). Experiments conducted at $[Ca^{2+}]_e \leq 50$ nM (i.e., slightly below $[Ca^{2+}]_i^{rest}$), adapted by 500 ms EGTA application to medium, before AED stimulation (0, 30, 80 ms). Note very rapid Ca redistribution already within 30 ms (= dead time of quenched-flow apparatus). Cytosolic [Ca] was registered at a distance of 0.5 μm from a trichocyst docking site. Mitochondria analyzed were also located in cell cortex. N (number of cells analyzed) = 5, 6, 6 (controls, 30 ms, 80 ms); n = 29, 31, 27 (**A**); 25, 29, 27 (**B**); 10, 11, 11 (**C**); bars = s.e.m.; * = statistically significant difference from control.

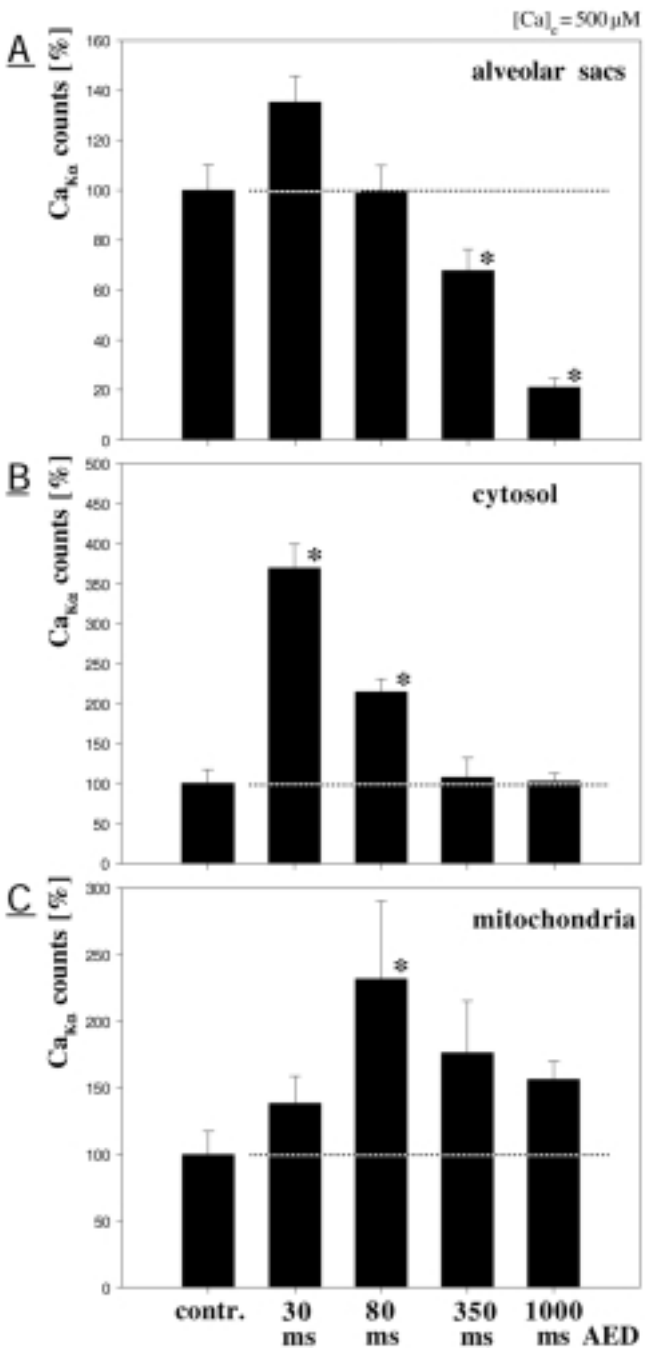

Fig. 5. Redistribution of Ca^{2+} during AED stimulation in presence of high $[Ca^{2+}]_e$ (= 500 µM). Note overshot of [Ca] in alveolar sacs at 30 ms, followed by a steady decay (**A**). Cytosolic [Ca] (0.5 µm from a trichocyst docking site) rapidly increases within 30 ms, and then decreases. Signal increase in cortical mitochondria follows that in cytosol with only little delay and culminates at 80 ms, followed by decrease within 350 ms and 1 s. Symbols as in Fig. 4. N = 9, 10, 9, 7, 8 (controls, 30 ms, 80 ms, 350 ms, 1 s); n = 50, 81, 84, 31, 36 (**A**); 51, 87, 67, 28, 36 (**B**); 21, 25, 18, 20, 28 (**C**).

were collected during 0.5 to 1 min floatation on 50 mM KF. Results thus achieved clearly reflect physiological data known from other analyses, i.e. the calcium storage capacity of ASs (see "Introduction"), as well as occurrence of cortical Ca^{2+} signals in electrophysiological (Erxleben and Plattner, 1994; Erxleben et al., 1997) and fluorochrome analyses (Klauke and Plattner, 1997). While these ESI data go far beyond any previous analysis, calibration was impossible, in contrast to this paper.

(ii) Which fraction of total calcium, free Ca^{2+} and/or protein-bound Ca is retained during freeze-substitution? Although this cannot be precisely determined, we can show retention of calcium in insoluble form, when freeze-substitution is executed in presence of highly soluble KF, from $-80\,^{\circ}C$ on. While in most other EDX analyses water was sublimated from sections by freeze-drying, we allowed fluoride ions (atomic weight = 19, i.e. similar to the molecular weight of water) to diffuse into frozen cells, while water was slowly substituted at the same temperature. In addition, we could show in a previous methodical paper (Hardt and Plattner, 1999) that calcium bound to a synthetic matrix (Chelex beads) is reliably retained without leakage and/or loss. This may correspond to the largely predominating percentage of calcium in ASs, where calcium will also exist predominately in bound form, just like in any other store (Plattner and Klauke, 2000). Any Ca^{2+} dissociating from binding sites will be rapidly trapped by the excess of fluoride, considering the low solubility of CaF_2, as it will occur also with strontium (Hardt and Plattner, 1999).

(iii) The sectioning protocol used for our present EDX analyses was the same as with our previous ESI analyses, but section thickness was 500 nm. Therefore, any diffusion/redistribution artifacts would be even much smaller than in high resolution ESI analyes in which we had found no evidence of such artifacts (Knoll et al., 1993).

(iv) Though in previous EDX analysis of paramecia, using freeze-dried sections, Schmitz and Zierold (1989) could register cortical $Ca_{K\alpha}$ signals, these could not be assigned to AS structures. This may be due not only to the fact that ASs were not recognized as calcium stores at that time, but even more to the notoriously poor structural resolution of such samples in the STEM-based EDX analysis. On the other hand, later elemental analysis of ASs by Stelly et al. (1995) was based on SIMS methodology whose elemental localization (resolution) is limited to several µm, whereas ASs are only ~0.1 µm wide. Moreover, in these studies ~20 s elapsed between AED stimulation and rapid freezing. In contrast, samples were quickly prepared for the present work. The ESI methodology used by Knoll et al. (1993) is not easily amenable to quantitation, in contrast to that used here, which simultaneously exploits the high temporal resolution of cryofixation and, thus, can reveal novel aspects.

(v) The value we determined for absolute total calcium, [Ca], in ASs of unstimulated cells is 43 mM ± 3.2 (s.e.m.). In the SR of skeletal muscle, Somlyo et al. (1981), using freeze-dried sections, determined [Ca] as 117 mM/kg dry weight, equivalent to ~33 mM (assuming 72% water content). Using a similar method, Schmitz and Zierold (1989) determined [Ca] in the "cytoplasm adjacent to pellicle" (bona fide regions containing ASs) as 267 mM/kg dry weight (±238, s.d.). Assuming a similar percentage of water content and considering the large statistical fluctuation of their data, these values are well within the frame of what we found (K. Zierold, personal communication).

In conclusion, we see several advantages of our current approach to study the rapid mobilization of calcium from ASs and its superposition by Ca^{2+} (or Sr^{2+}) influx at the same subsecond time scale as required for synchronous exocytosis.

Table II. Sr^{2+} can substitute for Ca^{2+} in *Paramecium* cultures, in long- (A) or short-term (B) experiments.

(A)	Cells → EGTA (5 s) → 0.01% AED, in variable $[Ca^{2+}]$ (a) Cells → EGTA (5 s) → 0.01% AED, in variable $[Sr^{2+}]$ (b)				
(a)			(b)		
[EGTA] (mM)	$[Ca^{2+}]$ (μM)	exocytosis	$[Sr^{2+}]$ (μM)	residual $[Ca^{2+}]$ (nM)	exocytosis
4.50	0.01	+	2.0	0.02	+
0.45	32.5	++	32.5	0.40	++
0.05	205.0	+++	211.0	13.9	+++

(B)	Cells → 4.5 mM EGTA (5 s) → $SrCl_2$ + 0.01% AED		
$[Sr]_{total}$ (mM)	$[Sr^{2+}]_{free}$ (mM)	residual $[Ca^{2+}]_{free}$ (μM)	exocytosis
0.1	0.004	0.05	+
1.0	0.08	0.08	++
2.5	0.72	0.43	++
10.0	8.0	4.22	+++

$[Ca^{2+}]$ and $[Sr^{2+}]$ were adjusted in the medium, by brief addition of EGTA before stimulation, to calculated values as indicated. Evaluation of exocytosis by light microscope analysis (see "Materials and methods"). (**A**) Adjustment of $[Ca^{2+}]_e$ to ~50 μM by EGTA allows for full exocytosis in response to AED (*a*). Long-time (12 h) substitution of Sr^{2+} for Ca^{2+} in medium (5 mM Pipes buffer, pH 7, + 1 mM KCl + $CaCl_2$ or $SrCl_2$, 1 mM each) shows that Sr^{2+} has no side-effects and can well support exocytosis (*b*). (**B**) Cells maintained for 12 h in 5 mM Pipes buffer, pH 7 (+ 1 mM KCl + 1 mM $CaCl_2$) were exposed to EGTA for 5 s and then to variable $[Sr^{2+}]$ in the 0.01% AED trigger solution to show that substitution of Sr^{2+} for Ca^{2+} supports exocytosis under conditions used for EDX analysis. Residual $[Ca^{2+}]$ is due to contamination by the calculated fraction of Ca^{2+} which is not chelated by EGTA. Sr^{2+} can support exocytosis, with trichocyst expulsion visible in the light microscope, even at residual $[Ca^{2+}]_e$ which per se would be too low (e.g., at $[Ca^{2+}]_e = 0.08$ μM, $[Sr^{2+}]_e = 80$ μM).

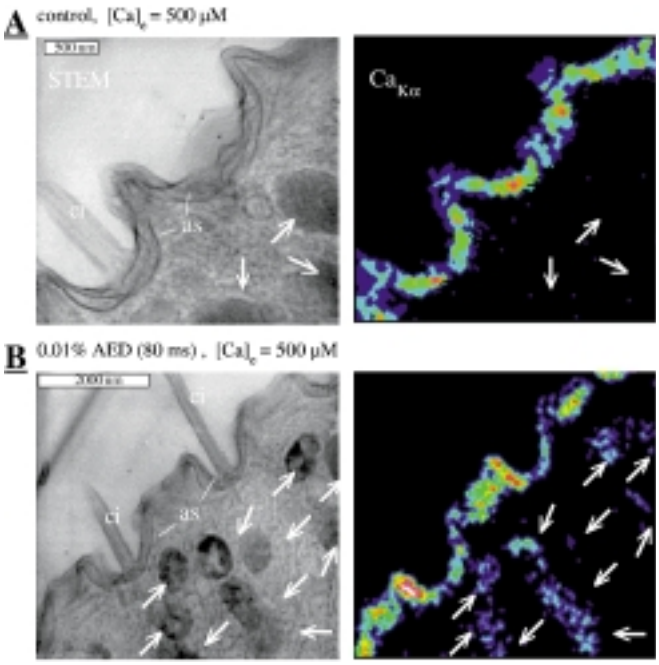

Fig. 6. Visualization by false-color imaging of rapid Ca^{2+} uptake into mitochondria. $Ca_{K\alpha}$ imaging before (**A**) or after AED stimulation for 80 ms (**B**) at $[Ca^{2+}]_e = 500$ μM. Note significant signal in alveolar sacs in (**A**) and in (**B**), in agreement with quantitative data shown in Fig. 5. In mitochondria, signals can be recorded only after stimulation (**B**). Note that mitochondria (*arrows*) in the $Ca_{K\alpha}$ image of the control cell (**A**) appear dark, whereas in the stimulated cell (**B**) they display a clear $Ca_{K\alpha}$ signal.

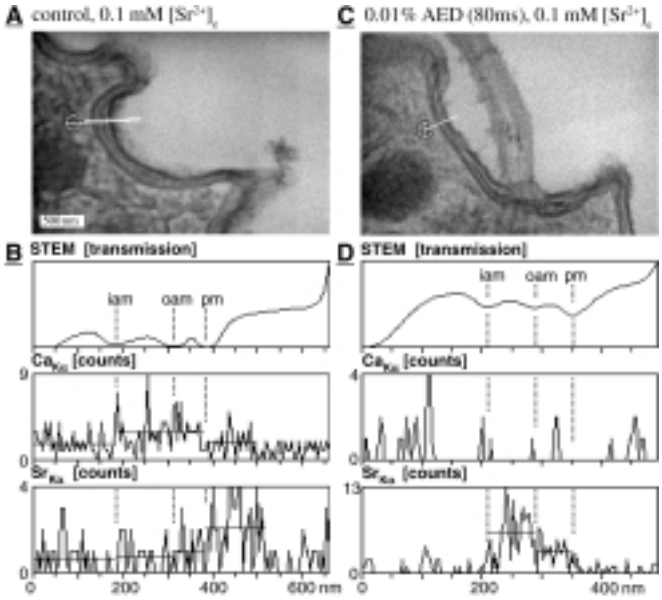

Fig. 7. Sr^{2+} influx rapidly replaces Ca in ASs during stimulation. Substitution of Ca^{2+} for Sr^{2+} in the medium for 80 ms, either without (**A**, **B**) or with 80 ms AED stimulation (**C**, **D**). Line scans starting at *asterisks* (**A**, **C**) were used in (**B**, **D**) to register STEM density profiles and to collect $Ca_{K\alpha}$ or $Sr_{K\alpha}$ signals (*boxes* from *top to bottom*). Without AED (**B**), the region between 200 and 400 nm, defined by inner and outer alveolar membrane (iam, oam) and plasma membrane (pm), displays some Ca signal, while Sr signals are abundant outside the plasma membrane (>400 nm), probably due to Sr binding to the glycocalyx. After AED stimulation (**D**), the Sr signal is enriched selectively in the alveolar sac region from where Ca signals have disappeared. This is indicated by the fact that, in the stimulated cell, Ca counts in the line scan across AS (**D**, *middle trace*) are low as compared to the unstimulated cell (**B**, *middle trace*). Note that Sr counts in the AS of the unstimulated and the stimulated cell (*lower trace* in (**B**) and (**D**)), measured simultaneously along the same axis, exhibit a reverse result. To eliminate unspecific mass thickness effects, signals were corrected for background as described in "Materials and methods"). Note that, although the contrast for iam, oam and pm in (**B**, **D**) is relatively low because density profiles were stretched to the same scale as used for the X-ray signals, spatial arrangement of these membranes can be clearly derived from the corresonding densitometric profile.

General biological implications

It has to be stressed that a transient Ca^{2+} influx from the extracellular medium into ASs is neither directed against a concentration gradient, nor does it include a reversal of the $[Ca^{2+}]$ gradient. This can be reasonably assumed since free calcium concentration in the extracellular medium, $[Ca^{2+}]_e = 500$ μM, will largely exceed that in ASs for the following reasons. We suggest that, just like in other stores, most of the

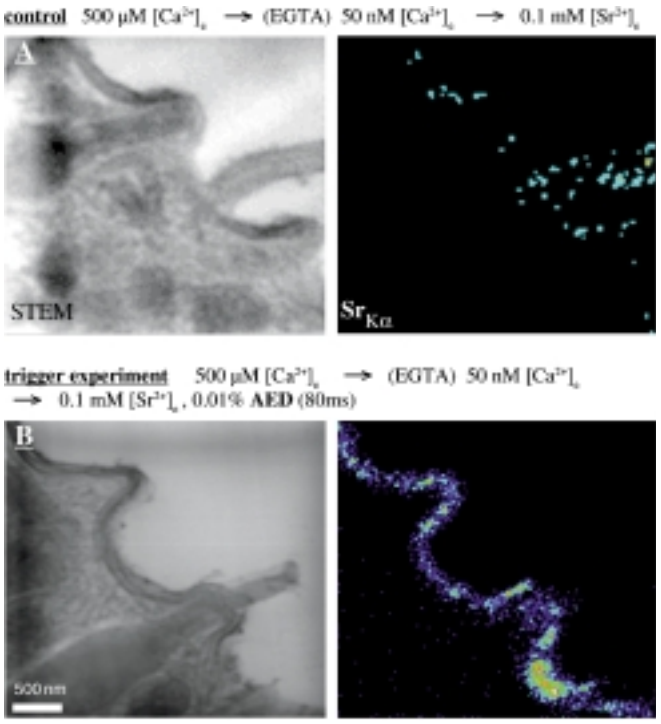

Fig. 8. Sr^{2+} influx rapidly replaces Ca in ASs during AED stimulation (false-color imaging). STEM and $Sr_{K\alpha}$ signals in $Ca_e^{2+} \rightarrow Sr_e^{2+}$ substitution experiments, either without stimulation (**A**) or after 80 ms AED stimulation (**B**), as indicated. Briefly, Ca_e^{2+} was chelated by EGTA and replaced by Sr^{2+} (with some residual Ca_e^{2+}) and cells were processed with/without AED stimulation as indicated. Note considerable increase of $Sr_{K\alpha}$ signals, after AED stimulation, in ASs over their entire extension.

alveolar Ca is bound to the calsequestrin-like protein which has been localized to ASs (Plattner et al., 1997b). The finding of $\sim$50 μM free Ca^{2+} in stores of some other systems (Miyawaki et al., 1997; Terraciano and MacLoed, 1997) or, more recently, of 10 μM in the ER of yeast (Strayle et al., 1999) matches well with our suggestion for paramecia, where we expect a similar low $[Ca^{2+}]$ level, though [Ca] is high in all these cases (see below). The fast release of Ca^{2+} from ASs during stimulation (Fig. 4), which appears to be the primary event after the AED stimulus, also has to be considered since this may contribute to a constant or even enlarged gradient (Miyawaki et al., 1997) that drives the transient Ca^{2+} influx into ASs, although the mechanism of fast coupling of both, intra- and extracellular pools, still has to be elucidated.

Estimates of $[Ca]_{total}$ in the SR and in the ER of different cells vary over a very wide range. Data reported by Meldolesi and Pozzan (1998) are between 5 to 50 mmoles/l (SR) and 5 to 10 mmoles/l (ER), respectively, as compared to $[Ca]_{total} =$ 43 mmoles/l in ASs. From a $[Ca]_{total} = 117$ mmoles/kg dry weight ($\sim$33 mmoles/l) in SR in a resting state, determined by EDX (Somlyo et al., 1981), 30% (Chen et al., 1996) or 40% are released per contraction cycle and 60% during tetanic stimulation (Kawai and Konishi, 1994). Similar data were obtained from photoreceptors during activation (Walz and Baumann, 1995). All this compares well with our present data. Also the subplasmalemmal $[Ca^{2+}]$ increment during SR mobilization (Tsugorka et al., 1995) is close to the half-width of 21 ms registered for Ca^{2+}-activated currents during AED stimulation (Erxleben et al., 1997). Yet no values comparable to those presented here are available for any other secretory system.

During 1 s AED stimulation we can clearly follow not only [Ca] changes in ASs, but also Ca spreading over exocytosis sites as well as rapid sequestration into cortical mitochondria. Although with restricted time resolution, sequestration of Ca^{2+} into mitochondria during stimulation has been observed in a variety of systems with widely different techniques (Horikawa et al., 1998; Rizzuto et al., 1998; Xu et al., 1997). A Ca^{2+} uniporter and a Na^+/Ca^{2+} exchanger system are discussed to mediate rapid Ca^{2+} uptake and release, respectively (Rutter et al., 1998; Csordás et al., 1999). We here show that mitochondria take up Ca^{2+} unexpectedly rapidly, followed by a slower release. The rapid uptake we find corresponds to the rule in mammalian cells that Ca^{2+} uptake by a Ca^{2+} uniporter responds most rapidly to Ca^{2+} pulse signals, with resetting within $\leq$1 s (Bernard, 1999). The rapid release we find suggests that mitochondria may only act as a transient Ca^{2+} buffer in our system.

Biological implications for our system and for related protozoa

We could establish $[Ca]_{total}$ in ASs and the percentage mobilized during AED stimulation. This allows for the following estimates. In AS, $[Ca]_{total}$ is 43 mmoles/l, and 52% are released during the 80 ms required for exocytosis. Theoretically Ca^{2+} could be dissipated over an entire cell volume of 0.73×10^{-10} l (Erxleben et al., 1997), but the primary site will be the suplasmalemmal space, occupying 161 μm^3, where Ca signals were registered by ESI (Knoll et al., 1993) and by electrophysiological recording of Ca^{2+}-activated currents (Erxleben and Plattner, 1994). There, $[Ca^{2+}] \sim 5$ μM is required for exocytosis (Klauke and Plattner 1997), while fluorochromes indicate a global $[Ca^{2+}]$ increase to only $\sim$0.3 μM. If our current EDX data were referred to the whole cell, a global increase to $[Ca]_{total} = 0.325$ mM would result, solely from ASs activation during AED stimulation. The discrepancy implies that cells operate with a large excess of Ca^{2+} to activate exocytosis, as has been discussed previouly for neuronal and endocrine systems (Chow et al., 1996; Henkel and Almers, 1996; Klingauf and Neher, 1997; Xu et al., 1997). It is now generally assumed that any calculated $[Ca^{2+}]$ increase is rapidly counteracted by Ca binding to endogenous cytosolic buffers, and by sequestration, of >98% of free Ca^{2+} (Chow et al., 1996). The ongoing depletion of Ca^{2+} from ASs (during 1 s) and Ca^{2+} influx from the medium beyond the time required for exocytosis (lasting 80 ms) may account for the requirement of increased $[Ca^{2+}]_i^{act}$ not only for exocytosis but also for exocytosis-coupled endocytosis (350 ms), as we conclude from previous experiments (Plattner et al., 1997a).

Mitochondria in *Paramecium* occupy a cytoplasmic volume fraction of $\sim 14 \pm 7\%$ (s.d., N = 20), representing 10.2×10^3 μm^3 (unpublished observation). From an average global increase of $[Ca]_{total}$ $\sim$1.2 mM (to be expected from store mobilization (this paper) and influx (Knoll et al., 1992)), 98% could maximally yield [Ca] = 85.7 mM in mitochondria (assuming they would take up all Ca). Since the [Ca] we register in mitochondria is about half this value at most, we conclude that "inactivation" of Ca^{2+} after stimulation takes place almost equally by mitochondrial sequestration and by cytosolic binding. Rapid clearing of Ca by mitochondria, e.g., in myocytes, was detected by EDX (Wendt-Gallitelli and Isen-

berg, 1991) and by fluorochrome analysis (Rizzuto et al., 1998; Rutter et al., 1998).

A $[Ca^{2+}]_i$ increase clearly also governs exocytosis of organelles of the "apicomplex" in *Toxoplasma gondii* during host cell invasion (Carruthers and Sibley, 1999), and similar mechanisms may apply to other members of Apicomplexans (Carruthers and Sibley, 1999; Ngo et al., 2000). However, a strict identification, localization, and functional analysis of Ca stores comparable to ASs remains to be established.

Conclusions

Our system seems to be faster than any other dense core vesicle exocytosis (see Kasai, 1999). We now showed by time-resolved EDX, including Sr^{2+}/Ca^{2+} exchange during quenched flow, that it involves a store-operated Ca^{2+} influx (SOC). This is in line with recent fluorochrome analyses by Klauke et al. (2000). There we have shown that ASs can be depleted of Ca^{2+} by a permeable mobilizing agent, 4-chloro-meta-cresol (which also releases Ca^{2+} from SR in muscle), in absence of Ca^{2+} in the medium, followed by increased rapid reuptake after readdition of Ca^{2+}. How our present data may be related to the release-activated Ca^{2+} transport (RACT) recently described in frog sympathetic neurons (Cseresnyés et al., 1997) or to any other mechanism still has to be established. The preparative approach we developed may also be useful for similar analyses in other cell types.

Acknowledgements. We thank Dr. W. C. DeBruijn (Rotterdam, The Netherlands) and BioRad (Munich, Germany) for providing Ca-exchange beads and Dr. J. A. Chandler (Cardiff, Wales, Great Britain) for help with the epoxy resin-based Ca standards, Dr. L. Reimer for calibration software, R. Bauer (Leo, Oberkochen, Germany) and Dr. Bauer (Oxford Instruments, Wiesbaden, Germany) for support in EDX analysis, as well as Actlabs (Ancaster, ONT, Canada) and Perkin-Elmer (Überlingen, Germany) for neutron activation analysis and atomic absorption spectrometry, respectively, which both helped us to control Ca standards. We are grateful to Ms. C. Hentschel for her help in some of the experiments, to Ms. S. Kolassa for preparing sections, to Dr. J. Hentschel for his help in some aspects of EM analysis and Ms. A. Keller for revising the English text. This study has been supported by Deutsche Forschungsgemeinschaft, grant Pl 78/15 and Pl 78/11 to H. Plattner (Schwerpunkt "Neue mikroskopische Methoden für Biologie und Medizin").

References

Anderegg, G. (1964): Komplexone XXXVI. Reaktionsenthalpie und -entropie bei der Bildung der Metallkomplexe der höheren EDTA-Homologen. Helv. Chim. Acta **47**, 1801 – 1814.

Barritt, G. J. (1999): Receptor-activated Ca^{2+} inflow in animal cells: a variety of pathways tailored to meet different intracellular Ca^{2+} signalling requirements. Biochem. J. **337**, 153 – 169.

Bernard, P. (1999): Mitochondrial transport of cations: channels, exchangers, and permeability transition. Physiol. Rev. **79**, 1127 – 1155.

Berridge, M. J. (1998): Neuronal calcium signaling. Neuron **21**, 13 – 26.

Bers, D. M., Patton, C. W., Nuccitelli, R. (1994): A practical guide to the preparation of Ca^{2+} buffers. Methods Cell Biol. **40**, 3 – 29.

Carruthers, V. B., Sibley, L. D. (1999): Mobililzation of intracellular calcium stimulates microneme discharge in *Toxoplasma gondii.* Mol. Microbiol. **31**, 421 – 428.

Chandler, J. A. (1976): A method for preparing absolute standards for quantitative calibration and measurement of section thickness with X-ray microanalysis of biological ultrathin specimens in EMMA. J. Microsc. (Oxford) **106**, 291 – 302.

Chen, W., Steenbergen, C., Levy, L. A., Vance, J., London, R. E., Murphy, E. (1996): Measurement of free Ca^{2+} in sarcoplasmic reticulum in perfused rabbit heart loaded with 1,2-bis(2-amino-5,6-difluorophenoxy)ethane-N,N,N′,N′-tetraacetic acid by ^{19}F NMR. J. Biol. Chem. **271**, 7398 – 7403.

Chow, R. H., Klingauf, J., Heinemann, C., Zucker, R. S., Neher, E. (1996): Mechanisms determining the time course of secretion in neuroendocrine cells. Neuron **16**, 369 – 376.

Clapham, D. E. (1995): Calcium signaling. Cell **80**, 259 – 268.

Cseresnyés, Z., Bustamante, A. I., Klein, M. G., Schneider, M. F. (1997): Release-activated Ca^{2+} transport in neurons of frog sympathetic ganglia. Neuron **19**, 403 – 419.

Csordás, G., Thomas, A. P., Hajnóczky, G. (1999): Quasi-synaptic calcium signal transmission between endoplasmic reticulum and mitochondria. EMBO J. **18**, 96 – 108.

DeBruijn, W. C. (1981): Ideal standards for quantitative X-ray microanalysis of biological specimens. Scanning Electron Microsc. **1981-II**, 357 – 367.

Dörge, A., Rick, R., Gehring, K., Thurau, K. (1978): Preparation of freeze-dried cryosections for quantitative X-ray microanalysis in biological soft tissues. Pflügers Arch. Eur. J. Physiol. **373**, 85 – 97.

Erxleben, C., Klauke, N., Flötenmeyer, M., Blanchard, M.-P., Braun, C., Plattner, H. (1997): Microdomain Ca^{2+} activation during exocytosis in *Paramecium* cells. Superposition of local subplasmalemmal calcium store activation by local Ca^{2+} influx. J. Cell Biol. **136**, 597 – 607.

Erxleben, C., Plattner, H. (1994): Ca^{2+} release from subplasmalemmal stores as a primary event during exocytosis in *Paramecium* cells. J. Cell Biol. **127**, 935 – 945.

Goodenough, R. D., Stenger, V. A. (1973): Magnesium, calcium, strontium, barium and radium. In: J. C. Bailar (ed): Comprehensive Inorganic Chemistry, Pergamon Press, Oxford, pp. 591 – 664.

Hall, T. A. (1979): Biological X-ray microanalysis. J. Microsc. (Oxford) **117**, 145 – 163.

Hardt, M., Plattner, H. (1999): Quantitative energy-dispersive X-ray microanalysis of calcium dynamics in cell suspensions during stimulation on a subsecond time scale: preparative and analytical aspects as exemplified with *Paramecium* cells. J. Struct. Biol. **128**, 187 – 199.

Hauser, K., Pavlovic, N., Kissmehl, R., Plattner, H. (1998): Molecular characterization of a sarco(endo)plasmic reticulum Ca^{2+}-ATPase gene from *Paramecium tetraurelia* and localization of its gene product to sub-plasmalemmal calcium stores. Biochem. J. **334**, 31 – 38.

Henkel, A. W., Almers, W. (1996): Fast steps in exocytosis and endocytosis studied by capacitance measurements in endocrine cells. Curr. Opin. Neurobiol. **6**, 350 – 357.

Horikawa, Y., Goel, A., Somlyo, A. P., Somlyo, A. V. (1998): Mitochondrial calcium in relaxed and tetanized myocardium. Biophys. J. **74**, 1579 – 1590.

Inesi, G., Sagara, Y. (1994): Specific inhibitors of intracellular Ca^{2+} transport ATPases. J. Membr. Biol. **141**, 1 – 6.

Kasai, H. (1999): Comparative biology of Ca^{2+}-dependent exocytosis: implications of kinetic diversity for secretory function. Trends Neurosci. **22**, 88 – 93.

Kawai, M., Konishi, M. (1994): Measurement of sarcoplasmic reticulum calcium content in skinned mammalian cardiac muscle. Cell Calcium **16**, 123 – 136.

Kerboeuf, D., Cohen, J. (1990): A Ca^{2+} influx associated with exocytosis is specifically abolished in a *Paramecium* exocytotic mutant. J. Cell Biol. **111**, 2527 – 2535.

Kissmehl, R., Huber, S., Kottwitz, B., Hauser, K., Plattner, H. (1998): Subplasmalemmal Ca-stores in *Paramecium tetraurelia*. Identification and characterisation of a sarco(endo)plasmic reticulum-like Ca^{2+}-ATPase by phosphoenzyme intermediate formation and its inhibition by caffeine. Cell Calcium **24**, 193 – 203.

Klauke, N., Blanchard, M.-P., Plattner, H. (2000): Polyamine triggering of exocytosis in *Paramecium* involves an extracellular Ca^{2+}/(polyvalent cation)-sensing receptor, subplasmalemmal Ca-store mobilization and store-operated Ca^{2+}-influx via unspecific cation channels. J. Membr. Biol. **174**, 141 – 156.

Klauke, N., Plattner, H. (1997): Imaging of Ca^{2+} transients induced in *Paramecium* cells by a polyamine secretagogue. J. Cell Sci. **110**, 975 – 983.

Klauke, N., Plattner, H. (1998): Caffeine-induced Ca^{2+} transients and exocytosis in *Paramecium* cells. A correlated Ca^{2+} imaging and quenched-flow/freeze-fracture analysis. J. Membr. Biol. **161**, 65 – 81.

Klingauf, J., Neher, E. (1997): Modeling buffered Ca^{2+} diffusion near the membrane: implications for secretion in neuroendocrine cells. Biophys. J. **72**, 674 – 690.

Knoll, G., Braun, C., Plattner, H. (1991): Quenched flow analysis of exocytosis in *Paramecium* cells: time course, changes in membrane structure, and calcium requirements revealed after rapid mixing and rapid freezing of intact cells. J. Cell Biol. **113**, 1295 – 1304.

Knoll, G., Grässle, A., Braun, C., Probst, W., Höhne-Zell, B., Plattner, H. (1993): A calcium influx is neither strictly associated with nor necessary for exocytotic membrane fusion in *Paramecium* cells. Cell Calcium **14**, 173 – 183.

Knoll, G., Kerboeuf, D., Plattner, H. (1992): A rapid calcium influx during exocytosis in *Paramecium* cells is followed by a rise in cyclic GMP within 1 s. FEBS Lett. **304**, 265 – 268.

Länge, S., Klauke, N., Plattner, H. (1995): Subplasmalemmal Ca^{2+} stores of probable relevance for exocytosis in *Paramecium*. Alveolar sacs share some but not all characteristics with sarcoplasmic reticulum. Cell Calcium **17**, 335 – 344.

Mackrill, J. J. (1999): Protein-protein interactions in intracellular Ca^{2+}-release channel function. Biochem. J. **337**, 345 – 361.

Meldolesi, J., Pozzan, T. (1998): The endoplasmic reticulum Ca^{2+} store: a view from the lumen. Trends Biochem. Sci. **23**, 10 – 14.

Meldolesi, J., Villa, A. (1993): Endoplasmic reticulum and the control of Ca^{2+} homeostasis. Subcell. Biochem. **21**, 189 – 207.

Metuzals, J., Chang, D., Hammar, K., Reese, T. S. (1997): Organization of the cortical endoplasmic reticulum in the squid giant axon. J. Neurocytol. **26**, 529 – 539.

Miyawaki, A., Llopis, J., Heim, R., McCaffery J. M., Adams, J. A., Ikura, M., Tsien, R. Y. (1997): Fluorescent indicators for Ca^{2+} based on green fluorescent proteins and calmodulin. Nature **388**, 882 – 887.

Montero, M., Alvarez, J., Scheenen, W. J. J., Rizzuto, R. Meldolesi, J., Pozzan, T. (1997): Ca^{2+} homeostasis in the endoplasmic reticulum: coexistence of high and low $[Ca^{2+}]$ subcompartments in intact HeLa cells. J. Cell Biol. **139**, 601 – 611.

Neher, E. (1998): Vesicle pools and Ca^{2+} microdomains: new tools for understanding their roles in neurotransmitter release. Neuron **20**, 389 – 399.

Ngo, H. M., Hoppe, H. C., Joiner, K. A. (2000): Differential sorting and post-secretory targeting of proteins in parasitic invasion. Trends Cell Biol. **10**, 67 – 72.

Plattner, H., Braun, C., Hentschel, J. (1997a): Facilitation of membrane fusion during exocytosis and exocytosis-coupled endocytosis and acceleration of "ghost" detachment in *Paramecium* by extracellular calcium. A quenched-flow/freeze-fracture analysis. J. Membr. Biol. **158**, 197 – 208.

Plattner, H., Habermann, A., Kissmehl, R., Klauke, N., Majoul, I., Söling, H.-D. (1997b): Differential distribution of calcium stores in *Paramecium* cells. Occurrence of a subplasmalemmal store with a calsequestrin-like protein. Eur. J. Cell Biol. **72**, 297 – 306.

Plattner, H., Klauke, N. (2000): Calcium in ciliated protozoa: Sources, regulation, and calcium-regulated cell functions. Int. Rev. Cytol. (in press).

Plattner, H., Lumpert, C. J., Knoll, G., Kissmehl, R., Höhne, B., Momayezi, M., Glas-Albrecht, R. (1991): Stimulus-secretion coupling in *Paramecium* cells. Eur. J. Cell Biol. **55**, 3 – 16.

Plattner, H., Stürzl, R., Matt, H. (1985): Synchronous exocytosis in *Paramecium* cells. IV. Polyamino compounds as potent trigger agents for repeatable trigger-redocking cycles. Eur. J. Cell Biol. **36**, 32 – 37.

Poenie, M., Epel, D. (1987): Ultrastructural localization of intracellular calcium stores by a new cytochemical method. J. Histochem. Cytochem. **35**, 939 – 956.

Putney, J. W. (1999): "Kissin' cousins": intimate plasma membrane-ER interactions underlie capacitative calcium entry. Cell **99**, 5 – 8.

Reimer, L. (1998): Scanning Electron Microscopy. Physics of Image Formation and Microanalysis. 2nd edn. Springer Verlag, Berlin, Heidelberg, New York.

Rizzuto, R., Pinton, P., Carrington, W., Fay, F. S., Fogarty, K. E., Lifshitz, L. M., Tuft, R. A., Pozzan, T. (1998): Close contacts with the endoplasmic reticulum as determinants of mitochondrial Ca^{2+} responses. Science **280**, 1763 – 1766.

Rutter, G. A., Fasolato, C., Rizzuto, R. (1998): Calcium and organelles: a two-sided story. Biochem. Biophys. Res. Commun. **253**, 549 – 557.

Schmitz, M., Zierold, K. (1989): X-ray microanalysis of ion changes during fast processes of cells, as exemplified by trichocyst exocytosis of *Paramecium caudatum*. In: H. Plattner (ed.): Electron Microscopy of Subcellular Dynamics, CRC Press, Boca Raton, FL, pp. 325 – 339.

Schwarzenbach, G., Senn, H., Anderegg, G. (1957): Komplexone XXVI. Ein großer Chelateffekt besonderer Art. Helv. Chim. Acta **40**, 1886 – 1890.

Somlyo, A. V., Gonzales-Serratos, H., Shuman, H., McClellan, G., Somlyo, A. P. (1981): Calcium release and ion changes in the sarcoplasmic reticulum of tetanized muscle: an electron-probe study. J. Cell Biol. **90**, 577 – 594.

Stelly, N., Halpern, S., Nicolas, G., Fragu, P., Adoutte, A. (1995): Direct visualization of a vast cortical calcium compartment in *Paramecium* by secondary ion mass spectrometry (SIMS) microscopy: possible involvement in exocytosis. J. Cell Sci. **108**, 1895 – 1909.

Stelly, N., Mauger, J. P., Kéryer, G., Claret, M., Adoutte, A. (1991): Cortical alveoli of *Paramecium*: a vast submembraneous calcium storage compartment. J. Cell Biol. **113**, 103 – 112.

Strayle, J., Pozzan, T., Rudolph, H. K. (1999): Steady-state free Ca^{2+} in the yeast endoplasmic reticulum reaches only 10 μM and is mainly controlled by the secretory pathway pump Pmr1. EMBO J. **18**, 4733 – 4743.

Terraciano, C. M. N., MacLoed, K. T. (1997): Measurements of Ca^{2+} entry and sarcoplasmic reticulum Ca^{2+} content during the cardiac cycle in guinea pig and rat ventricular myocytes. Biophys. J. **72**, 1319 – 1326.

Tse, F. W., Tse, A., Hille, B., Horstmann, H., Almers, W. (1997): Local Ca^{2+} release from internal stores controls exocytosis in pituitary gonadotrophs. Neuron **18**, 121 – 132.

Tsugorka, A., Ríos, E., Blatter, L. A. (1995): Imaging elementary events of calcium release in skeletal muscle cells. Science **269**, 1723 – 1726.

Walz, B., Baumann, O. (1995): Structure and cellular physiology of Ca^{2+} stores in invertebrate photoreceptors. Cell Calcium **18**, 342 – 351.

Warley, A. (1997): X-ray Microanalysis for Biologists. Portland Press, London, Miami, FL.

Wendt-Gallitelli, M. F., Isenberg, G. (1991): Total and free myoplasmic calcium during a contraction cycle: X-ray microanalysis in guinea-pig ventricular myocytes. J. Physiol. (London) **435**, 349 – 372.

Xu, T., Naraghi, M., Kang, H., Neher, E. (1997): Kinetic studies of Ca^{2+} binding and Ca^{2+} clearance in the cytosol of adrenal chromaffin cells. Biophys. J. **73**, 532 – 545.

Zhou, X. L., Chan, C. W. M., Saimi, Y., Kung, C. (1995): Functional reconstitution of ion channels from *Paramecium* cortex into artificial liposomes. J. Membr. Biol. **144**, 199 – 208.